Plant Omics Journal POJ

POJ 6(1):46-54 (2013) ISSN:1836-3644

In search for new players of the oxidative stress network by phenotyping an *Arabidopsis* T-DNA mutant collection on reactive oxygen species-eliciting chemicals

Veselin Petrov[1,2,*], Jos Schippers[3,4], Maria Benina[1,2], Ivan Minkov[1,2], Bernd Mueller-Roeber[3,4], Tsanko Gechev[1,2]

[1]Department of Plant Physiology and Molecular Biology, University of Plovdiv, 24 Tsar Assen str., Plovdiv 4000, Bulgaria
[2]Institute of Molecular Biology and Biotechnologies, 105 Ruski Blvd., Plovdiv 4000, Bulgaria
[3]Max Planck Institute of Molecular Plant Physiology, Am Muehlenberg 1, 14476 Potsdam, Germany
[4]Institute of Biochemistry and Biology, University of Potsdam, Karl-Liebknecht-Str. 24–25, 14476 Potsdam, Germany

***Corresponding author: vpetrov@plantgene.eu**

Abstract

The ability of some chemical compounds to cause oxidative stress offers a fast and convenient way to study the responses of plants to reactive oxygen species (ROS). In order to unveil potential novel genetic players of the ROS-regulatory network, a population of ~2,000 randomly selected *Arabidopsis thaliana* T-DNA insertion mutants was screened for ROS sensitivity/resistance by growing seedlings on agar medium supplemented with stress-inducing concentrations of the superoxide-eliciting herbicide methyl viologen or the catalase inhibitor 3-amino-triazole. A semi-robotic setup was used to capture and analyze images of the chemically treated seedlings which helped interpret the screening results by providing quantitative information on seedling area and healthy-to-chlorotic tissue ratios for data verification. A ROS-related phenotype was confirmed in three of the initially selected 33 mutant candidates, which carry T-DNA insertions in genes encoding a Ring/Ubox superfamily protein, ABI5 binding protein 1 (AFP1), previously reported to be involved in ABA signaling, and a protein of unknown function, respectively. In addition, we identified six mutants, most of which have not been described yet, that are related to growth or chloroplast development and show defects in a ROS-independent manner. Thus, semi-automated image capturing and phenotyping applied on publically available T-DNA insertion collections adds a simple means for discovering novel mutants in complex physiological processes and identifying the genes involved.

Keywords: growth; image analysis; methyl viologen; LemnaTec; screening; superoxide.
Abbreviations: ABI5 – ABA insensitive 5; AFP1 – ABI5 binding protein 1; AT – aminotriazole; MS medium – Murashige and Skoog medium; MV – methyl viologen; *nptII* – *neomycin phosphotransferase II*; PCD – programmed cell death; ROS – Reactive oxygen species; *YS1 – Yellow Seedlings 1*.

Introduction

Reactive oxygen species (ROS) such as hydrogen peroxide (H_2O_2), singlet oxygen ($^1O_2$) and superoxide radical ($O_2^{\bullet-}$), are inevitable toxic byproducts of aerobic way of life (Gadjev et al., 2008). In plants, the effects of ROS depend on their chemical identity, (sub-)cellular concentration, and duration of the concentration change (Gechev et al., 2002; Gechev et al., 2004). In low amounts they control an array of processes, including growth and development (Gapper and Dolan, 2006), immune reactions towards different plant pathogens (Apel and Hirt, 2004), seed germination (Schopfer et al., 2001), adaptation to a number of abiotic stress factors (Gill and Tuteja, 2010), etc. In contrast, in high doses ROS induce a physiological state denoted as oxidative stress, which is accompanied by a considerable reprogramming of cellular functions and may lead to activation of programmed cell death (PCD) pathways (Van Breusegem and Dat, 2006). Moreover, ROS accumulation causes significant damage to the cell due to the oxidation of DNA, RNA and proteins (Beckman and Ames, 1998). The relation between stress, ROS and PCD is of fundamental and practical importance, since many adverse environmental conditions, which cause major crop yield losses worldwide, stimulate ROS production and by this provoke PCD (Gechev et al., 2006). For example, during drought stress, which today is among the highest threats to crop production, intracellular ROS levels increase in C3 plants, mainly due to an enhancement of photorespiration, representing a major hazard for plant survival (Noctor et al., 2002). Despite the recent progress in our understanding of the molecular processes underlying ROS physiology and signaling in plants, major cellular players still remain to be characterized. This involves functional analysis,

for example of ROS-responsive transcriptional regulators (Maruta et al., 2012; Wu et al., 2012), ROS scavenging factors (Duan et al., 2012; Laporte et al., 2012), ROS sensors (Davletova et al., 2005; Hardin et al., 2009), and genes of currently unfamiliar molecular functions, but known to affect ROS tolerance, as for example reported for the *atr* genes (Gechev et al., 2008; Mehterov et al., 2012).

A convenient approach to study oxidative stress and/or PCD pathways is by treating plants with chemical agents that lead to ROS formation. Among the compounds having such features are aminotriazole (AT) and methyl viologen (MV; also called paraquat). AT is a potent inhibitor of catalase, an enzyme that catalyzes the conversion of H_2O_2 to water and oxygen (Margoliash and Novogrodsky, 1958; Margoliash et al., 1960); thus, plants treated with this toxin show severe PCD symptoms due to the elevation of intracellular H_2O_2 concentration. MV causes an accumulation of superoxide anions in chloroplasts, which arise when the partially reduced dipyridal cation is reoxidized by molecular oxygen (Hassan and Fridovich, 1978). Similarly to AT, MV also ultimately induces PCD. The properties of these herbicides were employed here for phenotype-based screening of *Arabidopsis thaliana* mutants by growing seedlings in culture medium supplemented with either AT or MV. This approach is technically simple and allows achieving a steady boost of ROS levels in the treated plants (Gechev et al., 2005), which provides a means for the identification of potential new players in the ROS or PCD signaling networks.

The phenotypic analysis of mutants still represents one of the most effective ways to explore gene functions (Sozzani and Benfey, 2011). Large collections of mutants are available for *Arabidopsis* and nearly every gene has been tagged by a T-DNA insertion. However, a complicated part during screening of a mutant collection remains the processing of large data sets, which is not only a time-consuming process, but may also be biased by the experimenter. To overcome this limitation, high-throughput phenotyping methods have recently been introduced to help molecular biologists and breeders perform rapid, reliable and non-destructive assessments of a variety of morphological and physiological parameters of large plant populations (Furbank and Tester, 2011). This is achieved through automated imaging in specifically designed stations that allow optimal light conditions and subsequent image processing/analysis by mathematical algorithms. Therefore, to increase the robustness of our approach, we used a previously established LemnaTec Scanalyzer HTS screening platform (Arvidsson et al., 2011) that automated the process of phenotype detection, provided a means to validate the phenotypes, increased the screening sensitivity and ultimately aided in the interpretation of the results.

The screening protocol was applied to a batch of ~2,000 randomly selected *Arabidopsis thaliana* T-DNA insertion lines from the SALK collection. Since in most cases these lines contain an insertion in a single genomic locus and the location of the T-DNA is preliminarily known (Alonso et al., 2003), tracking the gene causing an observed phenotype is relatively straightforward. A rescreen following the initial identification of a number of putative ROS-related mutants confirmed the phenotype of nine of them. Six mutants showed growth defects in an MV-independent manner, while the other three had an altered phenotype only on MV-containing medium, revealing previously uncharacterized elements of the ROS response network.

Results

Screen setup

In order to identify ROS-related mutants among the large set of lines, we first monitored the seedling area and the chlorotic lesions which appear when seedlings are grown on oxidative stress-inducing medium. In these conditions, ROS-sensitive mutants would have a delayed growth phenotype, mostly in combination with a reduced healthy/chlorotic tissue ratio when compared to the Col-0 wild-type controls. In contrast, ROS-tolerant mutants are expected to have a larger total area and less chlorotic tissues than the controls (i.e., a higher healthy/chlorotic tissue ratio). However, it is likely that the T-DNA collection also contains mutants that affect these parameters independently of oxidative stress. For example, mutants in house-keeping genes would differ from the wild type in total cotyledon/leaf area, while those impaired in chloroplast development would show an increased percentage of yellow tissues, similarly to the ROS-susceptible ones. Therefore, to discriminate between ROS-related and ROS-independent phenotypes the putative ROS mutants were rescreened both on MV/AT-containing as well as on standard MS medium (which does not induce stress). Although ROS-independent mutants were not in the main focus of this work, they might represent uncharacterized phenotypes of interest to the plant community in general. Under our growth conditions, the seedling responses to AT were much weaker (and often not discernable) than to MV, even at a higher concentration of AT (11 µM; data not shown). Therefore, we focused our further analysis on identifying mutants obtained on MV-containing medium.

Results of the primary screen and description of ROS-independent mutants

The initial screen of ~2,000 randomly chosen SALK lines led to the selection of 33 candidates which showed larger or smaller morphological differences in comparison to the wild-type Col-0 control. After rescreening in separate Petri dishes, the phenotype on ROS-inducing medium was confirmed for nine of the 33 SALK lines (Table 1). However, several of them also differed from the wild type on standard MS medium (i.e., in the absence of MV), indicating that the corresponding genes do not specifically participate in ROS-/senescence-associated processes. For example, the T-DNA insertion line SALK_015201 is characterized by a long-hypocotyl phenotype, which is independent of MV as the phenotype is also observed when plants are grown on MS control medium (Supplementary Fig. 1). Next to that, the last four mutants listed in Table 1 (SALK_002221; SALK_081796; SALK_118335; SALK_ 031707) appeared to be very sensitive in the initial MV screen, but had a very limited growth in optimal conditions as well. The affected genes are therefore likely to have housekeeping functions, leading to severe growth phenotypes when mutated. Indeed, according to the TAIR database (www.arabidopsis.org) three of them encode proteins localized in the chloroplast, of which one is involved in tyrosine biosynthesis (AT1G15710, impaired in SALK_081796) and another one is a plant-specific member of the dynamin superfamily that is essential for the

Table 1. Mutants isolated on MV-containing medium. The table includes information about the affected gene (according to TAIR10[a]), a description of the phenotype and the function of the encoded protein.

SALK entry	AGI code	Phenotype	Encoded protein[b]
SALK_015201	AT3G23900	long hypocotyl	RNA recognition motif (RRM)-containing protein
SALK_020158	AT1G69260	smaller on both AT and MV	ABI five binding protein 1 (AFP1); involved in: abscisic acid mediated signaling
SALK_123515	AT3G22690	completely bleached on AT and MV	pentatricopeptide repeat (PPR)-containing protein
SALK_099042	AT4G39140	severe damage on MV	protein binding / zinc ion binding; involed in: N-terminal protein myristoylation
SALK_113517	AT2G41830	severe damage on MV	unknown protein
SALK_002221	AT5G22090	severe damage on MV	protein of unknown function, located in chloroplast
SALK_081796	AT1G15710	severe damage on MV	prephenate dehydrogenase family protein
SALK_118335	AT1G03160	severe damage on MV	member of the dynamin superfamily of membrane remodeling GTPases that regulates organization of the thylakoid network
SALK_031707	AT3G49560	severe damage on MV	mitochondrial inner membrane translocase subunit Tim17/Tim22/Tim23 family protein

[a]TAIR database website: http://www.arabidopsis.org/index.jsp.
[b]Other useful databases: http://ppdb.tc.cornell.edu and http://bioinformatics.psb.ugent.be/plaza

normal structure and function of the thylakoid network (AT1G03160, mutated in SALK_118335) (Gao et al., 2006). The identification of the SALK_118335 line shows that the screen for yellowing not only works for characterizing the chlorotic effects caused by MV treatment but also allows the finding of leaf greening mutants. The line SALK_002221 possesses a T-DNA insertion in the uncharacterized gene AT5G22090, whose protein product is also targeted to the chloroplast, but has an unknown function. The fourth mutant in this group, SALK_031707, is defective in AT3G49560, predicted to encode an import translocase Tim17/Tim22/Tim23 family member involved in protein transport through the inner mitochondrial membrane.

Finally, the SALK_123515 mutant appeared completely bleached in the initial screening on both AT and MV (Fig. 1, Panel A). However, a following search in the literature revealed that the mutant has already been characterized (Zhou et al., 2009). The gene affected, *Yellow Seedlings 1* (*YS1*), participates in the control of leaf greening during early leaf development where it is required for chloroplast formation. Although *YS1* knockouts were slightly smaller when cultivated in the presence of MV compared to control conditions, we did not consider this phenotype caused by MV treatment alone.

Novel players in the Arabidopsis ROS-network - The lines SALK_099042 and SALK_113517 showed the most drastic phenotypes on MV-containing medium in the primary screen (Fig. 1B, C). Quantitative analyses with the LemnaGrid software confirmed that both of them were considerably smaller than the wild-type controls (approximately 3.6 times for SALK_099042 seedlings and 3.8 times for SALK_113517) and seemed severely stressed on the 7th day after germination, as revealed by the ratio of green/yellow tissues (Fig. 2). As it can be seen from the figure, plants of the line SALK_099042 had on average ~87% chlorotic tissues, whilst this was only ~41% for the wild type. Initially, the mutants in well A3 of the same plate also displayed a sensitive phenotype (Fig. 2), but this could not be confirmed in a following experiment. Similarly to SALK_099042, the percentage of chlorotic tissues in SALK_113517 was 93%, which is an indicator of serious damage at this concentration of MV. The same results were obtained in the second round of screening for both SALK_099042 and SALK_113517. Importantly, in the absence of MV the mutants had a phenotype comparable to that of the wild-type plants. As these lines likely represent genuine ROS mutants impaired in processes that maintain ROS homeostasis, we selected them for further characterization. There is currently no information on the putative function of the gene AT2G41830, which is affected in SALK_113517. The line SALK_099042 possesses a T-DNA insertion in the RING/U-box superfamily member gene AT4G39140, which has multiple splice variants, one of which is a possible target of N-terminal myristoylation (Boisson et al., 2003). As the functions of both genes are not yet well characterized, the cellular mechanisms underlying ROS sensitivity in the mutants are currently unknown.

Finally, the line SALK_020158 initially showed a lower seed germination rate compared to the other mutants and therefore could not be reliably assessed with the LemnaGrid software, despite the fact that the plants were phenotypically similar to SALK_099042 and SALK_113517. However, the subsequent rescreen in individual dishes confirmed the susceptibility of SALK_020158 seedlings to oxidative stress (Fig. 3). Unlike the previous two candidates, this line carries an insertion in a gene which is already well studied - *ABI5 binding protein 1* (*AFP1*), known to be a negative regulator of the ABA insensitive 5 (ABI5) transcription factor (Lopez-Molina et al., 2003).

Analysis of mutant zygosity

An important initial step in the analysis of a T-DNA insertion mutant is the confirmation of its homozygosity (Ulker et al., 2008). Even though the pROK2 vector, used for the creation of the SALK mutant collection, contains the selectable marker gene *nptII* (*neomycin phosphotransferase II*), transgene silencing sometimes obscures reliable selection of mutants on kanamycin (Daxinger et al., 2008). Moreover, the *nptII* marker and the insertion in the target gene are not necessarily genetically linked (Ulker et al., 2008). To confirm homozygosity of our seed stocks of SALK_099042, SALK_113517 and SALK_020158 lines, we performed PCR-based genotyping conducted with two different pairs of primers, to allow easy identification of wild-type plants (used as positive control), and homo- or heterozygous mutants. Initially, the lines SALK_113517 and SALK_020158 were homozygous, while

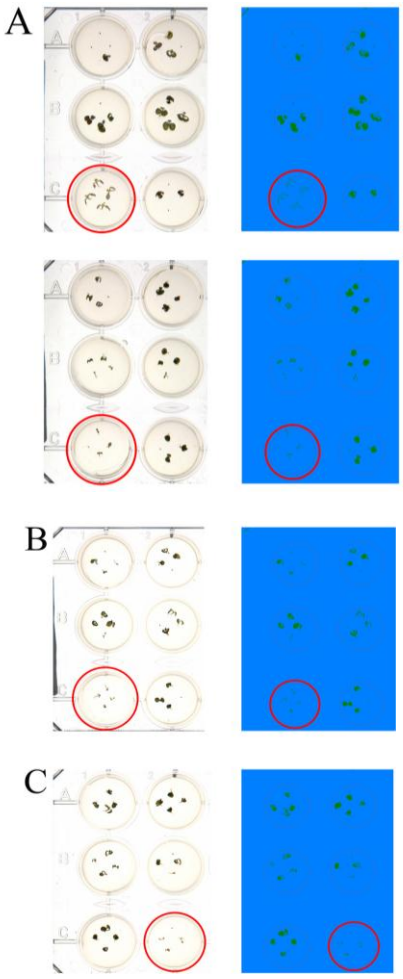

Fig 1. Mutant phenotypes. In panels A, B, and C, mutants with phenotypes (red encircled) are presented together with other T-DNA insertion lines that do not show a prominent phenotype under the screening conditions on day 7 after germination. Panel A: Yellow Seedlings 1 (YS1) mutant. Plants were grown on either AT-containing medium (upper images) or MV-containing medium (lower images). Panel B: Line SALK_099042 grown on MV-containing medium. Panel C: SALK_113517 grown on MV-containing medium. In A, B and C, photographs on the left were made in normal light, while photographs on the right show the discrimination of healthy/chlorotic tissues, revealed by employing a user-made image processing algorithm embedded in the LemnaGrid environment; the tool assigns each pixel from the seedling area to one of two possible categories – healthy tissue (green colour) or chlorotic tissue (yellow colour). The chlorotic tissues on these pictures are shown in blue as the background for a better contrast.

both homo- and heterozygous mutants were found in the SALK_099042 population used for screening (data not shown). The fact that homo- and heterozygous individuals had the same phenotype indicates a dominant nature of the SALK_099042 mutation or that the observed phenotype is caused by a mutation in another locus. Only plants homozygous for the T-DNA insertion were used for seed harvesting and their progeny was genotyped again to confirm that subsequent physiological experiments will be carried out with homozygous offspring of the three lines (Supplementary Fig. 2).

In summary, the screening of ~2,000 T-DNA insertion mutants yielded three potential new players involved in ROS-regulation: *AFP1* (AT1G69260); the unknown protein encoded by the AT2G41830 gene; and the Ring/U box superfamily protein from the AT4G39140 locus. None of these genes has so far been implicated in oxidative stress signaling. Their phenotypes on MS medium supplemented with 0.5 µM MV are presented in Figure 3. The structure, exon/intron composition and location of the T-DNAs are shown in Figure 4. As it can be seen, according to the TAIR database in all instances the T-DNA insertion is actually positioned in introns; in the case of AT4G39140, the intron is located within the 5' UTR. After sequencing from the left border of the inserted T-DNA, this was confirmed for AT1G69260 and AT4G39140. However, the sequencing data demonstrated that in the line SALK_113517, the T-DNA is integrated not in the AT2G41830 intron shown in TAIR, but in the adjacent 3' exon (Figure 4).

Discussion

The effects of oxidative stress on cellular metabolism and physiology can be assessed by treating plants with ROS-inducing chemical agents (Gechev et al., 2004; Mahalingam et al., 2006) or by employing mutants with e.g. compromised antioxidant systems (op den Camp et al., 2003; Rizhsky et al., 2003; Vanderauwera et al., 2005). In our search for novel players in the *Arabidopsis* ROS network we combined both methods by growing randomly selected T-DNA insertion lines on medium supplemented with MV or AT. In the past, approaches that employed MV as a trigger for ROS production were mainly used to look for ROS-tolerant mutants (Carroll et al., 1988; Fujibe et al., 2004; Chen et al., 2009). Since our goal included the identification of MV-sensitive mutants as well, we applied a relatively low MV concentration (0.5 µM), which in our culture conditions was high enough to cause detectable damage to *Arabidopsis* seedlings, without killing them. In contrast, although AT has been proposed as a convenient pharmacological inhibitor for studying H_2O_2-induced processes (Gechev et al., 2005), to our knowledge no large-scale screening with AT for resistant or susceptible mutants has been performed so far. However, most of the lines we screened displayed a much weaker phenotype on AT (even at 11 µM) than on MV, which was possibly due to the light source used in our experiments.

Another novelty presented in this study was the utilization of an automated image capturing system which by virtue of an integrated image processing algorithm allows a rapid quantification of cotyledon/leaf area and healthy-to-chlorotic (green-to-yellow) ratios of seedlings grown in multiwell plates. Manual phenotyping of large sets of plants is normally quite laborious and requires an appreciable amount of time and expertise. An automated screening platform may thus aid to rapidly compare a larger number of genotypes and

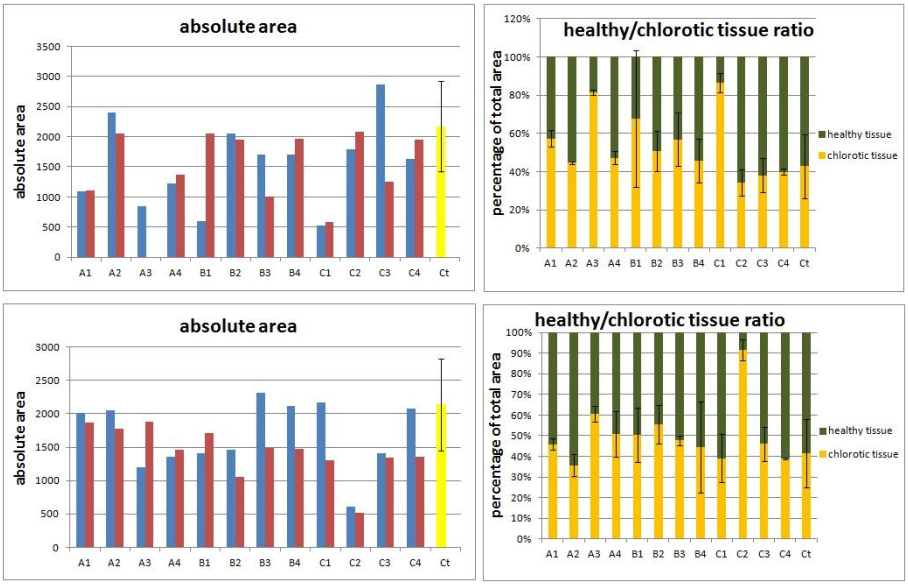

Fig 2. Quantification of the absolute area (in pixel^2) and the healthy-to-chlorotic tissue ratio of mutant seedlings and wild-type controls grown on MV-containing MS medium. Each chart contains 13 objects, of which ´Ct´ represents the Col-0 wild-type control, while the other 12 represent different mutants grown in the wells of the tissue culture plate (A1 - A4, B1 - B4, C1 - C4). In the absolute area charts shown on the left, the average object areas per well from each of the duplicate plates (see *Materials and methods*) were plotted next to each other for each of the mutants. For Col-0 wild-type seedlings means ± SD were calculated from six different wells. In the charts on the right, the average healthy-to-chlorotic tissue ratios determined for each well of the duplicate plates are shown on the same column (± SD).

A) Quantitative results for SALK_099042 (well C1) and other T-DNA insertion lines.

B) Quantitative results for SALK_113517 (well C2) and other T-DNA insertion lines.

provide the possibility for a precise quantification and evaluation of the analyzed traits. Moreover, it has the potential of detecting weaker phenotypes which would be hardly distinguishable by unassisted visual inspection. Previously, the LemnaTec Scanalyzer HTS system was successfully applied for integrated image processing of plants at the rosette leaf stage of development; up to 7,000 individual plants could be screened per day with a very low (< 2%) technical variance using the setup reported (Arvidsson et al., 2011). Herein, our goal was to extend this pipeline to screening of mutant seedlings. Indeed, the automated imaging system allowed the processing of a few dozens of multiwell plates per hour, which accelerated the characterization of individual mutants. However, despite the precision of the measurements performed with the LemnaTec platform, the overall variance of the data was considerably higher than for plants at the rosette stage (Arvidsson et al., 2011). One of the main reasons was the high biological variability of the measured parameters (the total area and the ratio of healthy to chlorotic tissues) of the control seedlings (Fig. 2). In addition, the relatively low number of seedlings examined per T-DNA insertion line (up to eight in total, with maximum four seedlings grown in individual wells) further boosted the variance. Moreover, due to the transparency of the MS agar medium used for seedling growth, the homogeneity of the light field in the camera chamber had a major impact on the calculation of healthy-to-chlorotic tissue ratios (see *Materials and methods*). As a consequence, each irregularity in the light field influenced the discrimination of the green and yellow colour categories. Due to these limitations, the automated LemnaTec system was not suitable to identify weaker mutants with the same high efficiency that we previously reported for rosette-stage plants. However, the massive image data accumulated with the LemnaTec setup were useful for the unbiased verification of the phenotypes of the manually chosen mutants.

The screening of ~2,000 SALK mutants ultimately resulted in the identification of three candidates with ROS-related phenotypes. Two of them (SALK_099042 and SALK_113517) possess a T-DNA insertion in genes which have not been characterized yet and are currently difficult to link to ROS metabolism. However, the third mutant, SALK_020158, is affected in the *AFP1* gene, which functions in ABA signaling (Lopez-Molina et al., 2003), but for which a role in ROS signaling or tolerance has not been previously reported. At the early post-germination stage young seedlings possess an adaptive mechanism to sustain water deficit, which is manifested as a reversible growth arrest induced by ABA or salt stress and requires the action of the ABI5 transcription factor (Lopez-Molina et al., 2001). The growth arrest efficiency is dependent on the level of ABI5, which can be negatively regulated by the AFP1 protein to attenuate the ABA signal (Lopez-Molina et al., 2003). AFP1 executes this negative control by targeting ABI5 for ubiquitin-mediated degradation. Previously, *afp1* mutants were shown to be more sensitive to ABA and salt stress than wild-type plants (Lopez-Molina et al., 2003; Garcia et al., 2008). We speculate that ROS accumulation triggers an ABI5-mediated growth arrest and that *afp1* seedlings are unable to escape from it due to no or little AFP1 to block the signal. The further physiological characterization

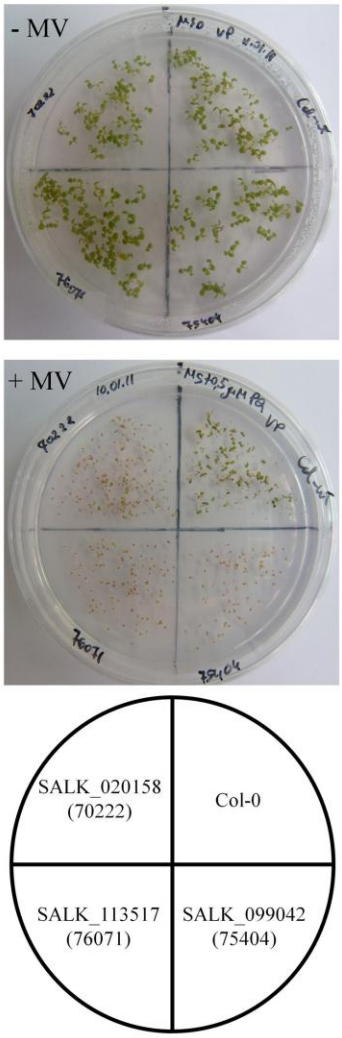

Fig 3. Seedling phenotypes on MS medium with or without MV. Upper panel: MS medium. Central panel: MS medium supplemented with 0.5 µM MV. Lower panel: Schematic presentation of the growth sectors of the Col-0 wild type and the three SALK mutants. Images were taken on day 4 after germination. Note the higher sensitivity of the SALK mutants to MV, compared to the wild-type control.

of the SALK_020158 mutant may lead to new insights into the mode of action of AFP1 and provide a link between the ROS and ABA pathways.

Taken together, we describe here a protocol for the systematic screen of an *Arabidopsis* T-DNA collection using a semi-automated setup. The main advantage of this approach is that the experimenter directly receives a quantifiable phenotype, which in most cases is caused by an easily traceable defective locus. It resulted in the identification of three genes that remained undiscovered in previous screens for ROS-related phenotypes. In addition, we report six further mutants related to growth and chloroplast development, most of which have not been described yet. Thus, by extending the MV screening approach reported here to the entire set of available T-DNA insertion lines or even other types of mutants, many novel ROS-resistant or -sensitive mutants are likely to be discovered in the near future.

Materials and methods

Plant material and growth conditions

Arabidopsis thaliana (L.) Heynh. was used in all experiments. Seeds of ~8,000 SALK lines were initially obtained from the Nottingham Arabidopsis Stock Centre (NASC; http://arabidopsis.info) and propagated at the Max Planck Institute of Molecular Plant Physiology (Potsdam-Golm, Germany) for further analysis. The collection includes mutants which in most cases have a single mapped T-DNA insertion within a gene body or promoter, allowing rapid identification of the genotype underlying a specific phenotype. For *in vitro* cultivation, seeds were sown on standard Murashige and Skoog (MS) agar-containing medium, supplemented or not with methyl viologen or 3-amino-1,2,4-triazole (Sigma-Aldrich, St. Louis, MO, USA). Seedlings of mutants and the Col-0 wild-type control were grown in a Percival CU-36L5 growth chamber (Percival Scientific, Iowa, USA) at 21°C, 150 µmol $m^{-2}s^{-1}$ light intensity, a 16 h light/8 h dark photoperiod, and 70% relative humidity.

Oxidative stress treatments

Approximately two thousand *Arabidopsis* T-DNA insertion lines were randomly chosen from the entire set of lines and screened for sensitivity or resistance on oxidative stress-inducing MS medium. Seeds were surface-sterilized in 75% ethanol for 5 min and then sown in Greiner Cellstar® 12-well tissue culture plates (Greiner Bio-one GmbH, Frickenhausen, Germany) with MS medium containing either 9 µM AT or 0.5 µM MV, with one line per well (4 seedlings per line in each well). These toxin concentrations were chosen after a preliminary experiment with a gradient of different levels of both AT (5, 7, 9, and 11 µM) and MV (0.4, 0.5, 0.6, and 0.7 µM), whose purpose was to determine the conditions in which Col-0 seedlings develop clear sub-lethal symptoms of stress and PCD. Each line was tested in two duplicate plates for each of the herbicides. Before transferring to optimal light and temperature conditions, plates were incubated at 4°C for three days to break any residual dormancy.

Phenotype evaluation

Phenotypes were scored seven days after germination both visually and by analyzing the plates by the software provided together with the image capturing instrument (LemnaGrid). Images were taken using an automated system provided with a top view camera manipulated by a robotic arm (Basler scout scA1600-14gc, Basler AG, Ahrensburg, Germany, www.baslerweb.com) in a cabinet with optimal light control (Scanalyzer HTS, LemnaTec, Wuerselen, Germany, www.lemnatec.com) equipped with a barcode reader for the identification of individual plates. Photographs were analyzed on the basis of two variables – the total object area (in $pixel^2$) and the ratio of healthy (green)/chlorotic (yellow) tissues. The reason for choosing the healthy/chlorotic tissue ratios as an indicator of the level of ROS-related stress is the fact that ROS

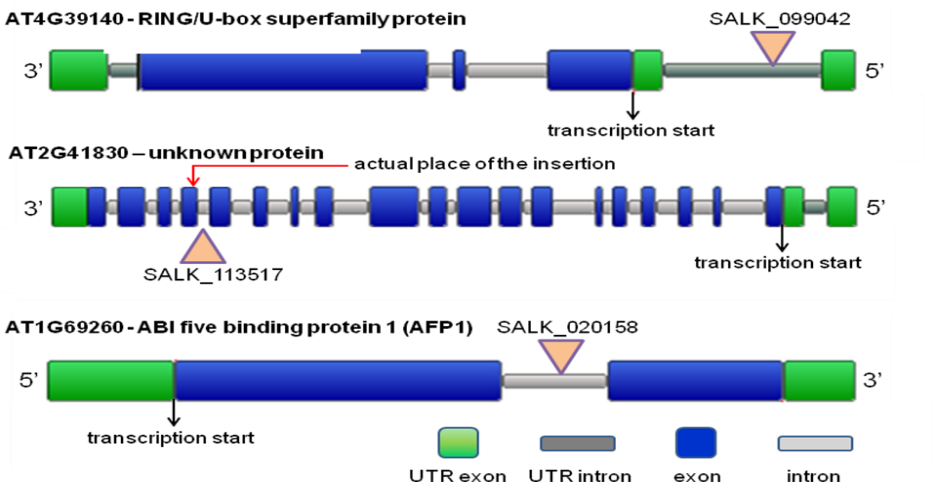

Fig 4. T-DNA insertion points in the three ROS-sensitive mutants identified (SALK_099042, SALK_113517, SALK_020158). The schemes were taken from the PLAZA database (Proost et al., 2009; Van Bel et al., 2012) (http://bioinformatics.psb.ugent.be/plaza), and were slightly modified. The triangles present the insertions as shown in the TAIR database. For the gene AT2G41830, the red arrow demonstrates the actual place of insertion, which is in the adjacent 3' exon, as determined by sequencing from the left border of the T-DNA.

accumulation is associated with the onset of PCD, which in turn causes chlorosis that can be easily and reliably scored by the available software. To obtain this parameter, images were processed through a user-made algorithm in the LemnaGrid environment, which assigns each pixel from the seedling area to one of two possible categories – healthy tissue (green colour) or chlorotic tissue (yellow colour). The discrimination between the two colour categories is automatically carried out after RGB channel weighting and comparison to a set of 15 nuances of both green and yellow which was created in advance by photographing 7-day-old seedlings on standard MS (without MV; for green) or on MS + 0.7 µM MV (for yellow) medium.

PCR genotyping of mutants

All samples for DNA extraction were flash-frozen in liquid nitrogen and subsequently ground to fine powder using a Retsch CryoMill (www.retsch.com). DNA was isolated using a modification of the original CTAB protocol (Murray and Thompson, 1980). PCR reactions for genotyping mutants were performed in 25 µl total volume using a recombinant *Taq* polymerase (0.75 units per reaction; Life Technologies, Carlsbad, CA, USA), 100 ng genomic DNA template, 1 x PCR buffer supplied by the same company, 1.5 mM $MgCl_2$, 0.2 mM each of the four dNTPs, and 0.2 µM forward/reverse primers. The applied PCR program included an initial incubation for 5 min at 94°C; then 30 cycles of: denaturation at 94°C for 30 s, primer annealing at 60°C for 30 s and fragment elongation at 72°C for 45 s; and a final extension at 72°C for 5 min.

For each line, two reactions with two different primer combinations were conducted. The first primer combination (with primers annealing on both sides of the predicted T-DNA insertion site) leads to a PCR product when a wild-type allele is present. The second primer combination generates an amplicon only when a T-DNA insertion is present in at least one allele of the analyzed gene, since one of the primers targets a region near the left border of the T-DNA while the other anneals to an adjacent genomic sequence. The list of primers used is given in Supplementary Table 1.

Acknowledgements

We thank Dr. Karin Koehl and her Green Team from the Max Planck Institute of Molecular Plant Physiology for propagating the SALK lines and excellent plant care. We thank the Nottingham Arabidopsis Stock Center (NASC; http://arabidopsis.info) for providing seeds of the T-DNA insertion lines. This work was financially supported by EC FR7 (project Biosupport, 245588).

References

Alonso JM, Stepanova AN, Leisse TJ, Kim CJ, Chen H, Shinn P, Stevenson DK, Zimmerman J, Barajas P, Cheuk R, Gadrinab C, Heller C, Jeske A, Koesema E, Meyers CC, Parker H, Prednis L, Ansari Y, Choy N, Deen H, Geralt M, Hazari N, Hom E, Karnes M, Mulholland C, Ndubaku R, Schmidt I, Guzman P, Aguilar-Henonin L, Schmid M, Weigel D, Carter DE, Marchand T, Risseeuw E, Brogden D, Zeko A, Crosby WL, Berry CC, Ecker JR (2003) Genome-wide insertional mutagenesis of *Arabidopsis thaliana*. Science. 301:653-657

Apel K, Hirt H (2004) Reactive oxygen species: metabolism, oxidative stress, and signal transduction. Annu Rev Plant Biol. 55:373-399

Arvidsson S, Perez-Rodriguez P, Mueller-Roeber B (2011) A growth phenotyping pipeline for *Arabidopsis thaliana* integrating image analysis and rosette area modeling for robust quantification of genotype effects. New Phytol. 191:895-907

Beckman KB, Ames BN (1998) Mitochondrial aging: open questions. Ann NY Acad Sci. 854:118-127

Boisson B, Giglione C, Meinnel T (2003) Unexpected protein families including cell defense components feature in the N-myristoylome of a higher eukaryote. J Biol Chem. 278:43418-43429

Carroll EW, Schwarz OJ, Hickok LG (1988) Biochemical Studies of Paraquat-Tolerant Mutants of the Fern *Ceratopteris richardii*. Plant Physiol. 87:651-654

Chen R, Sun S, Wang C, Li Y, Liang Y, An F, Li C, Dong H, Yang X, Zhang J, Zuo J (2009) The *Arabidopsis* PARAQUAT RESISTANT2 gene encodes an S-nitrosoglutathione reductase that is a key regulator of cell death. Cell Res. 19:1377-1387

Davletova S, Rizhsky L, Liang H, Shengqiang Z, Oliver DJ, Coutu J, Shulaev V, Schlauch K, Mittler R (2005) Cytosolic ascorbate peroxidase 1 is a central component of the reactive oxygen gene network of *Arabidopsis*. Plant Cell. 17:268-281

Daxinger L, Hunter B, Sheikh M, Jauvion V, Gasciolli V, Vaucheret H, Matzke M, Furner I (2008) Unexpected silencing effects from T-DNA tags in *Arabidopsis*. Trends Plant Sci. 13:4-6

Duan M, Feng HL, Wang LY, Li D, Meng QW (2012) Overexpression of thylakoidal ascorbate peroxidase shows enhanced resistance to chilling stress in tomato. J Plant Physiol. 169:867-877

Fujibe T, Saji H, Arakawa K, Yabe N, Takeuchi Y, Yamamoto KT (2004) A methyl viologen-resistant mutant of *Arabidopsis*, which is allelic to ozone-sensitive rcd1, is tolerant to supplemental ultraviolet-B irradiation. Plant Physiol. 134:275-285

Furbank RT, Tester M (2011) Phenomics - technologies to relieve the phenotyping bottleneck. Trends Plant Sci. 16:635-644

Gadjev I, Stone JM, Gechev TS (2008) Programmed cell death in plants: new insights into redox regulation and the role of hydrogen peroxide. Int Rev Cell Mol Biol. 270:87-144

Gao H, Sage TL, Osteryoung KW (2006) FZL, an FZO-like protein in plants, is a determinant of thylakoid and chloroplast morphology. Proc Natl Acad Sci USA. 103:6759-6764

Gapper C, Dolan L (2006) Control of plant development by reactive oxygen species. Plant Physiol. 141:341-345

Garcia ME, Lynch T, Peeters J, Snowden C, Finkelstein R (2008) A small plant-specific protein family of ABI five binding proteins (AFPs) regulates stress response in germinating *Arabidopsis* seeds and seedlings. Plant Mol Biol. 67:643-658

Gechev T, Gadjev I, Van Breusegem F, Inze D, Dukiandjiev S, Toneva V, Minkov I (2002) Hydrogen peroxide protects tobacco from oxidative stress by inducing a set of antioxidant enzymes. Cell Mol Life Sci. 59:708-714

Gechev TS, Ferwerda MA, Mehterov N, Laloi C, Qureshi MK, Hille J (2008) *Arabidopsis* AAL-toxin-resistant mutant atr1 shows enhanced tolerance to programmed cell death induced by reactive oxygen species. Biochem Bioph Res Co. 375:639-644

Gechev TS, Gadjev IZ, Hille J (2004) An extensive microarray analysis of AAL-toxin-induced cell death in *Arabidopsis thaliana* brings new insights into the complexity of programmed cell death in plants. Cell Mol Life Sci. 61:1185-1197

Gechev TS, Minkov IN, Hille J (2005) Hydrogen peroxide-induced cell death in *Arabidopsis*: transcriptional and mutant analysis reveals a role of an oxoglutarate-dependent dioxygenase gene in the cell death process. IUBMB Life. 57:181-188

Gechev TS, Van Breusegem F, Stone JM, Denev I, Laloi C (2006) Reactive oxygen species as signals that modulate plant stress responses and programmed cell death. Bioessays. 28:1091-1101

Gill SS, Tuteja N (2010) Reactive oxygen species and antioxidant machinery in abiotic stress tolerance in crop plants. Plant Physiol Bioch. 48:909-930

Hardin SC, Larue CT, Oh MH, Jain V, Huber SC (2009) Coupling oxidative signals to protein phosphorylation via methionine oxidation in *Arabidopsis*. Biochem J. 422:305-312

Hassan HM, Fridovich I (1978) Superoxide radical and the oxygen enhancement of the toxicity of paraquat in *Escherichia coli*. J Biol Chem. 253:8143-8148

Laporte D, Olate E, Salinas P, Salazar M, Jordana X, Holuigue L (2012) Glutaredoxin GRXS13 plays a key role in protection against photooxidative stress in *Arabidopsis*. J Exp Bot. 63:503-515

Lopez-Molina L, Mongrand S, Chua NH (2001) A postgermination developmental arrest checkpoint is mediated by abscisic acid and requires the ABI5 transcription factor in *Arabidopsis*. Proc Natl Acad Sci USA. 98:4782-4787

Lopez-Molina L, Mongrand S, Kinoshita N, Chua NH (2003) AFP is a novel negative regulator of ABA signaling that promotes ABI5 protein degradation. Genes Dev. 17:410-418

Mahalingam R, Jambunathan N, Gunjan SK, Faustin E, Weng H, Ayoubi P (2006) Analysis of oxidative signalling induced by ozone in *Arabidopsis thaliana*. Plant Cell Environ. 29:1357-1371

Margoliash E, Novogrodsky A (1958) A study of the inhibition of catalase by 3-amino-1:2:4:-triazole. Biochem J. 68:468-475

Margoliash E, Novogrodsky A, Schejter A (1960) Irreversible reaction of 3-amino-1:2:4-triazole and related inhibitors with the protein of catalase. Biochem J. 74:339-348

Maruta T, Noshi M, Tanouchi A, Tamoi M, Yabuta Y, Yoshimura K, Ishikawa T, Shigeoka S (2012) H_2O_2-triggered retrograde signaling from chloroplasts to nucleus plays specific role in response to stress. J Biol Chem. 287:11717-11729

Mehterov N, Balazadeh S, Hille J, Toneva V, Mueller-Roeber B, Gechev T (2012) Oxidative stress provokes distinct transcriptional responses in the stress-tolerant *atr7* and stress-sensitive *loh2 Arabidopsis thaliana* mutants as revealed by multi-parallel quantitative real-time PCR analysis of ROS marker and antioxidant genes. Plant Physiol Bioch. 59:20-29

Murray MG, Thompson WF (1980) Rapid isolation of high molecular weight plant DNA. Nucleic Acids Res. 8:4321-4325

Noctor G, Veljovic-Jovanovic S, Driscoll S, Novitskaya L, Foyer CH (2002) Drought and oxidative load in the leaves of C3 plants: a predominant role for photorespiration? Ann Bot. 89:841-850

op den Camp RG, Przybyla D, Ochsenbein C, Laloi C, Kim C, Danon A, Wagner D, Hideg E, Gobel C, Feussner I, Nater M, Apel K (2003) Rapid induction of distinct stress responses after the release of singlet oxygen in *Arabidopsis*. Plant Cell. 15:2320-2332

Proost S, Van Bel M, Sterck L, Billiau K, Van Parys T, Van de Peer Y, Vandepoele K (2009) PLAZA: a comparative genomics resource to study gene and genome evolution in plants. Plant Cell. 21:3718-3731

Rizhsky L, Liang H, Mittler R (2003) The water-water cycle is essential for chloroplast protection in the absence of stress. J Biol Chem. 278:38921-38925

Schopfer P, Plachy C, Frahry G (2001) Release of reactive oxygen intermediates (superoxide radicals, hydrogen peroxide, and hydroxyl radicals) and peroxidase in germinating radish seeds controlled by light, gibberellin, and abscisic acid. Plant Physiol. 125:1591-1602

Sozzani R, Benfey PN (2011) High-throughput phenotyping of multicellular organisms: finding the link between genotype and phenotype. Genome Biol. 12:219

Ulker B, Peiter E, Dixon DP, Moffat C, Capper R, Bouche N, Edwards R, Sanders D, Knight H, Knight MR (2008) Getting the most out of publicly available T-DNA insertion lines. Plant J. 56:665-677

Van Bel M, Proost S, Wischnitzki E, Movahedi S, Scheerlinck C, Van de Peer Y, Vandepoele K (2012) Dissecting plant genomes with the PLAZA comparative genomics platform. Plant Physiol. 158:590-600

Van Breusegem F, Dat JF (2006) Reactive oxygen species in plant cell death. Plant Physiol. 141:384-390

Vanderauwera S, Zimmermann P, Rombauts S, Vandenabeele S, Langebartels C, Gruissem W, Inze D, Van Breusegem F (2005) Genome-wide analysis of hydrogen peroxide-regulated gene expression in *Arabidopsis* reveals a high light-induced transcriptional cluster involved in anthocyanin biosynthesis. Plant Physiol. 139:806-821

Wu A, Allu AD, Garapati P, Siddiqui H, Dortay H, Zanor MI, Asensi-Fabado MA, Munne-Bosch S, Antonio C, Tohge T, Fernie AR, Kaufmann K, Xue GP, Mueller-Roeber B, Balazadeh S (2012) JUNGBRUNNEN1, a reactive oxygen species-responsive NAC transcription factor, regulates longevity in *Arabidopsis*. Plant Cell. 24:482-506

Zhou W, Cheng Y, Yap A, Chateigner-Boutin AL, Delannoy E, Hammani K, Small I, Huang J (2009) The *Arabidopsis* gene YS1 encoding a DYW protein is required for editing of rpoB transcripts and the rapid development of chloroplasts during early growth. Plant J. 58:82-96